JOURNAL OF MATERIALS SCIENCE 27 (1992) 2117–2123

# Exploitation of a pulsed neutron source for the structural study of anisotropic polymer films

G. R. MITCHELL, R. CYWINSKI
*J.J. Thomson Physical Laboratory and Polymer Science Centre, University of Reading, Whiteknights, Reading RG6 2AF, UK*

A novel but simple time-of-flight neutron scattering geometry which allows structural anisotropy to be probed directly, simultaneously and thus unambiguously in polymeric and other materials is described. A particular advantage of the simultaneous data collection when coupled to the large area of the beam is that it enables thin films ($< 10\ \mu m < 10$ mg) to be studied with relative ease. The utility of the technique is illustrated by studies on both deformed poly(styrene) glasses and on thin films of electrical conducting polymers. In the latter case, the power of isotopic substitution is illustrated to great effect. The development of these procedures for use in other areas of materials science is briefly discussed.

## 1. Introduction

Neutron scattering is a well known and well used probe of the structural properties of bulk samples of materials [1–5]. Neutrons are not only far more penetrating than X-rays, they are also scattered as strongly by light elements as by heavy ones. It is this feature that facilitates the characterization of the structural organization of organic materials, including polymeric systems. Moreover, the technique of isotopic substitution, wherein specific elemental components of the sample are selectively replaced by isotopes with profoundly different scattering lengths, can provide a unique and unambiguous solution for the structure under investigation. In polymer science, the technique of isotopic substitution has been used extensively to evaluate the dimensions of the polymer chain trajectories using small-angle, or more precisely low-$Q$, neutron scattering [6]. Little (if any) use has been made of neutron facilities in determining smaller-scale structures in polymers through the use of so-called wide-angle scattering techniques, even though these procedures have been widely and successfully exploited in the study of inorganic glasses, molecular liquids and other materials [1, 4, 7]. Evaluation of structures using wide-angle neutron scattering generally requires the preparation of samples weighing several grams. However, many materials of scientific and technological interest are prepared in the form of thin and thick films, for example semiconductors, coatings, and organic films for non-linear optics, and it is the atomic or molecular organization within these films that is to be evaluated. Such films are usually too thick for electron microscopy without involved preparation. But what can be achieved with neutron scattering when only several mg of such films are available? Moreover, how can the structural organization of such films be determined when the structure is expected to be intrinsically anisotropic or highly disordered? We focus on the exploitation of the particular features of time-of-flight neutron scattering through a simple but novel scattering geometry which enables the measurement of the anisotropic structure of thin-film samples. The procedure we have developed is illustrated first with results obtained from a bulk sample of poly(styrene). We then demonstrate the power of the approach with an investigation of electrically conducting polymer films, of less than 10 μm in thickness and weighing less than 10 mg, in which isotopic substitution is employed to great effect. Finally, the potential applications of this novel technique are discussed in a wider context.

## 2. Structure and neutron scattering

The intensity measured in a neutron-scattering experiment is, in part, proportional to the differential cross section, $d\sigma/d\Omega$, which is in turn directly related to the Fourier transform of the atomic pair-wise correlation functions. We can write for a system of $N$ atoms the differential cross-section [2, 3]

$$\frac{d\sigma}{d\Omega} = \left\{\sum_{n}^{N}\sum_{m}^{N} b_n b_m \exp i[\boldsymbol{Q}(\boldsymbol{r}_n - \boldsymbol{r}_m)]\right\} \quad (1)$$

Here $b_n$ and $b_m$ are the scattering amplitudes of the nuclei positioned at $\boldsymbol{r}_n$ and $\boldsymbol{r}_m$, respectively and $i = \sqrt{-1}$. $\boldsymbol{Q}$ is the scattering vector, or the difference between the wave vectors of the incident and scattered neutron. The magnitude of $\boldsymbol{Q}$, for elastic scattering, is defined as

$$Q = \frac{4\pi\sin\theta}{\lambda} \quad (2)$$

where $\lambda$ is the neutron wavelength, and $\theta$ is half scattering angle. It should be noted that Equation 1 can be separated into two components: the self correlation terms, for which $n = m$, resulting in an incoherent background containing no spatial information; and the pairwise terms for which $n \neq m$. It is

0022–2461 

these latter terms which are of principal interest. There are many routes to the analysis of such a differential cross section, for example through its calculation from model structures [7, 8], by Fourier transform to obtain the radial or cylindrical distribution functions [8, 9] or by more simple inspection and comparison. Moreover, it is evident that the observed cross section can be substantially modified by selective replacement of isotopes with differing $b$ at specific positions $\boldsymbol{r}$. The most widely used isotopic substitution, and one of particular interest in studies of organic materials, is that of deuterium ($b = 6.674 \times 10^{-15}$ m) for hydrogen ($b = 3.740 \times 10^{-15}$ m). Not only does this substitution offer a tremendous contrast in scattering amplitude at the hydrogen sites, it also substantially reduces the spin-incoherent scattering cross section, arising from the interaction between the neutron and the proton spin, from 80 to 2 barns per atom.

The possibility of isotopic substitution provides a powerful structural tool. However, when considering the generality of the technique it should be remembered that for many materials, total or selective deuteration is far from being a simple chemical technique. For many aromatic-based polymer systems, the monomer or polymer may be totally deuterated by proton exchange in acidic conditions [10]. However, for saturated aliphatic systems, and for selective deuteration, the chemistry may have to start with relatively simple units which are then built up into the monomers and polymers [11]. In these cases the complexity of the chemical synthesis will need to be weighed carefully against the structural information which may be accessed.

## 3. Neutron scattering using a pulsed source

In a conventional X-ray or neutron elastic-scattering experiment, a monochromatic beam of wavelength $\lambda$ is incident on the sample, and the scattered intensity is recorded as a function of the angle of scatter, $2\theta$, as indicated in Fig. 1a. To measure the $Q$-dependence of the intensity over a reasonable range of scattering vector, a wide angular range of $2\theta$ is required. This is generally achieved by moving a single detector sequentially through $2\theta$, or by employing a more complex wide-angle position-sensitive detector. When such scattering measurements are made on anisotropic samples, the angle, $\alpha$, between the scattering vector, $Q$, and the symmetry axis of the sample will change as the scattering angle is varied. In the case of a single detector this can be overcome by rotating the sample by $\theta$ as the detector position is changed by $2\theta$. In such cases the scattering vector remains in a fixed plane and therefore the angle between $Q$ and $\alpha$ may be varied easily [12]. In the case of a position-sensitive detector, a $\theta$–$2\theta$ rotation can similarly be used, but only if the high count rates afforded by such a detector are sacrificed; in essence the detector is then used almost as a single channel device. Instead of selecting $\boldsymbol{Q}$ by means of a fixed wavelength and variable $\theta$, the neutron time-of-flight technique uses a fixed scattering angle and a broad range of incident wavelengths [4, 5] as indicated in Fig. 1b. A white neutron beam is produced in a burst at time $t = 0$. The time taken for a neutron of velocity $v$ to reach the detector at a distance $L$ from the source is

$$t = \frac{L}{v} = CL\lambda \tag{3}$$

where $C$ is a constant, which for $t$ in ms, $L$ in m and $\lambda$ in nm takes the value 0.025278. We can therefore write

$$\boldsymbol{Q} = \frac{4\pi CL\sin\theta}{t} \tag{4}$$

$\boldsymbol{Q}$ can therefore be defined by simply time sorting the neutrons as they arrive at a detector. The total $Q$ range available is restricted only by the minimum measurable time-of-flight (in principle governed by the response time of the detector) and the maximum time-of-flight, which is defined by the time interval between bursts of neutrons from the source. The essence of the time-of-flight technique is thus that at a single scattering angle, $2\theta$, the $\boldsymbol{Q}$-dependent intensity can be measured over a broad $Q$ range without moving the detector and with the same angular relationship between the sample's symmetry axis and the scattering vector. With several detectors positioned around the sample at different scattering angles, a complete map of the scattered intensity as a function of both $\boldsymbol{Q}$ and $\alpha$ may therefore be obtained simultaneously. This is illustrated in Fig. 2, using as an example the detector arrangement of the liquid and amorphous materials diffractometer (LAD) at ISIS the Rutherford Appleton Laboratory's pulsed neutron spallation source [13]. It should be noted that the $\boldsymbol{Q}$ resolution available on a time-of-flight scattering spectrometer is governed by both the time resolution and geometrical considerations, such as collimation, and detector and sample size. At moderate distances from the neutron source (10–12 m) the geometrical and time contributions are approximately equal, and lead to a constant fractional resolution in $\boldsymbol{Q}$. While the time resolution can be improved by extending the total flight path, $L$, this also leads to an increase in the minimum $Q$ available at a particular detector position, due to frame overlap

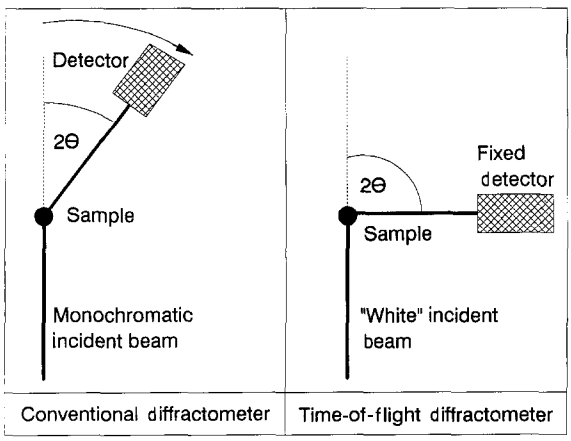


*Figure 1* A schematic representation of a conventional fixed wavelength, variable angle diffractometer and of the fixed angle time-of-flight technique.

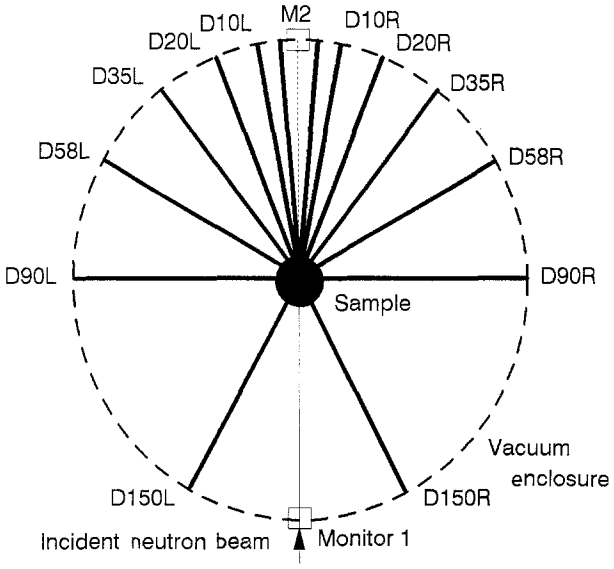


*Figure 2* Layout of the detectors on the LAD diffractometer at ISIS.

effects. This latter effect arises since slow neutrons from one pulse will reach the detector after the second pulse has been initiated, and thus any time synchronization is lost.

## 4. Experimental techniques

### 4.1. Neutron facility

The experiments performed in this study were carried out at ISIS [14]. The heart of ISIS is a synchrotron ring which accelerates protons to an energy of 800 MeV. Bursts of protons of this energy, and of 0.6 μs duration, are extracted at a frequency of 50 Hz and transported to a depleted uranium target where high-energy neutrons are produced by the process of spallation. These high-energy neutrons are of little use in scattering experiments. They are therefore moderated, a process of limited thermalization which reduces the neutron energies from the MeV to the more useful meV range. Although the very short pulse duration of 0.6 μs is sacrificed through moderation, the moderator design limits broadening of the pulse to the range 1–50 μs. The time zero signal, which triggers the time-of-flight sorting of neutrons arriving at the detector, is derived from the current pulse associated with protons striking the target. A consequence of the pulsed structure of the neutron beam, and the moderation process, is that the number of neutrons incident on the sample is strongly time-(i.e. wavelength-) dependent. This time dependence is adequately accounted for by monitoring the intensity of the beam with a low-efficiency detector before it reaches the sample.

### 4.2. Instrumentation

The results presented in this report were obtained using the POLARIS powder diffractometer [15] and the LAD [13]. Both instruments have a total (target-to-detector) path length of approximately 12 m. This distance, together with a maximum measurable time-of-flight allowed by the pulse repetition period of 20 ms, governs the minimum $Q$ that can be accessed in any one of the detectors positioned around the sample. For example, for the detectors situated at $2\theta = +/-90°$, which are of particular importance in this study, $Q_{min} \sim 13\ nm^{-1}$. The wavelength-dependent efficiency of the detectors on POLARIS and LAD, and the wavelength variation of the incident flux, were corrected for by using a sample of vanadium sheet of similar dimensions to the sample under investigation. Vanadium has a coherent scattering amplitude of almost zero, but scatters strongly and isotropically with a cross section of $5.1/4\pi$ barns steradian$^{-1}$ atom$^{-1}$, through the isotopic spin-incoherent process, thereby providing an essentially $Q$-independent scattering calibrant. If desired, the known vanadium scattering cross-section may be used to place the sample scattering on an absolute scale. Absorption and multiple-scattering corrections were found to be insignificant for the thin samples considered here, and thus were not made.

Fig. 2 shows schematically the range of scattering angles available. Two detectors are of particular value and interest as shown in Fig. 3, which illustrates a simple but highly effective geometry allowing the scattering to be recorded simultaneously for the situation in which $Q$ is parallel to a symmetry axis of the sample, and for $Q$ perpendicular to that axis. This is achieved by placing the sample at 45° to the incident beam and utilizing the + 90° and the − 90° detectors. This mode of operation allows simultaneous data accumulation and hence avoids the need to move or rotate the sample, in addition to considerably reducing the time required for the complete experiment. In principle, such an arrangement would allow the evolution of anisotropy to be measured *in situ* in real-time, for example, for liquid-crystal systems in electric or magnetic fields, or for stress fields applied to polymeric materials. Practically, these possibilities are currently limited by the incident flux and the detector solid angle.

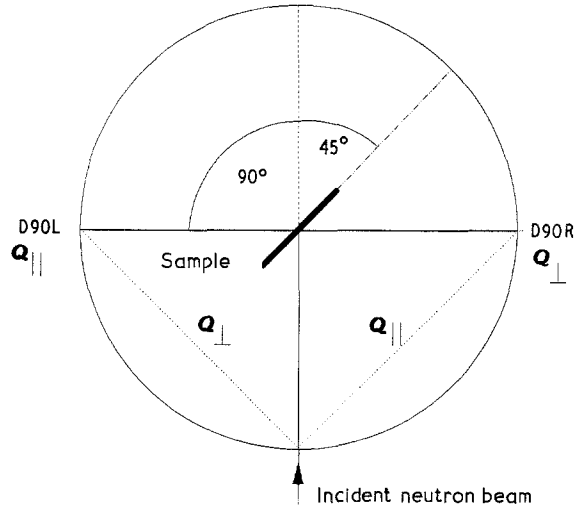


*Figure 3* The essentials of the sample and scattering geometry which allows simultaneous measurement of scattering patterns with $Q$ parallel to the sample axis and $Q$ perpendicular to the sample surface.

### 4.3. Materials

Two types of polymeric material were used in these exploratory studies. The first was an example of a glass-forming non-crystalline polymer in which the molecular orientation introduced during deformation in the melt may be preserved by rapidly cooling into the glassy state [16]. An aligned sample of fully deuterated poly(styrene) synthesized through a melt polymerization technique using 1 mol % of AIBN (azo bis-isobutyro nitrile) and $C_8D_8$ (Aldrich) as the initiator at 55 °C was prepared by extrusion in a small channel die held at a temperature just above the glass transition. By this technique, a sample $10 \times 10 \times 1$ mm was extruded to give an extension ratio of 2.0.

The second group of materials considered were thin films of electrically conducting polymers based on poly(pyrrole). These films of area $15 \times 40$ mm were prepared electrochemically by a one-step oxidative polymerization procedure [17]. The materials so prepared contain both the polymer and dopant units. These dopant units are present in high concentrations, typically one dopant unit for three to four pyrrole rings. It is perhaps more appropriate to consider the material as a salt with the dopant units, for example $ClO_4^-$, $SO_4^{2-}$ and toluene sulphonate, as the anions. At these concentrations it is not surprising that the type of dopant unit has a significant impact on both electrical and mechanical properties. Initial X-ray scattering studies suggest that under certain conditions [18, 19] films with an anisotropic molecular structure may be prepared. In this study we have examined poly(pyrrole) films prepared using $ClO_4^-$, $SO_4^{2-}$ and toluene sulphonate as the dopants. Full details of the sample preparation are given elsewhere [20].

## 5. Experimental results

Fig. 4 shows the scattering curve obtained using LAD for an undeformed sample of deuterated poly(styrene) at room temperature. These data were obtained in the 20° detector bank. The data illustrate one of the many advantages of time-of-flight neutron scattering, namely the large $Q$ range from 2–240 $nm^{-1}$. The data are similar to the published X-ray scattering data [16, 21], but of course such X-ray data only extend over a limited $Q$ range and diminish in intensity at high $Q$ values because of the $Q$-dependent X-ray scattering factors. A detailed analysis of the X-ray scattering data [16] showed that the diffuse peak at $Q \sim 8\,nm^{-1}$ arises from correlations between neighbouring phenyl groups which form stacks or so-called superchains. This peak is particularly sensitive to temperature. The diffuse peaks at higher scattering vectors arise principally from correlations within individual chain segments, and thus can provide information regarding the chain conformations. The availability of scattering data over a large $Q$ range should aid such analysis, and a detailed study is in progress (B. Rosi and G. R. Mitchell [22]).

Fig. 5 shows the scattering intensity measured for the deformed sample using the $+/-90°$ detectors with sample positioned at 45° to the incident beam. A consequence of the use of these higher angle detectors is that the minimum $Q$ accessible increases from $2\,nm^{-1}$ to $13\,nm^{-1}$. From these two curves, one obtained with $Q$ parallel to the extension axis and the other with $Q$ perpendicular to that axis, it can be seen that the poly(styrene) sample possesses an anisotropic molecular organisation. The level and sign of the anisotropy vary with the scattering vector: at high values of $Q$, say $> 100\,nm^{-1}$, there is minimal anisotropy. This is simply a consequence of the fact that as $Q$ increases, the scattering pertains more to locally defined distances such as C–C distances, which have a greater degree of structural isotropy than the large scale correlations such as those between neighbouring phenyl rings. We have plotted the ratio of the two curves obtained with $Q$ parallel and perpendicular to the extrusion direction as a function of $Q$ in Fig. 6. This shows more clearly the variation in the anisotropy of the scattering. The dashed part of the curve is from data obtained by using the 20° detector bank and positioning the sample at 10° and 80° to the incident beam. The data in Fig. 6 show that the diffuse

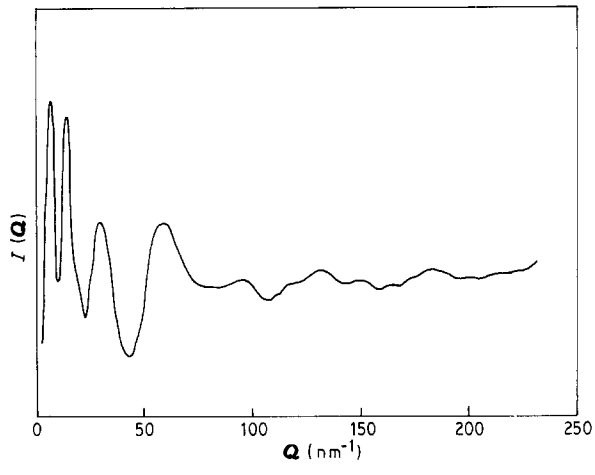


*Figure 4* The scattering data recorded using LAD for an isotropic sample of fully deuterated poly(styrene).

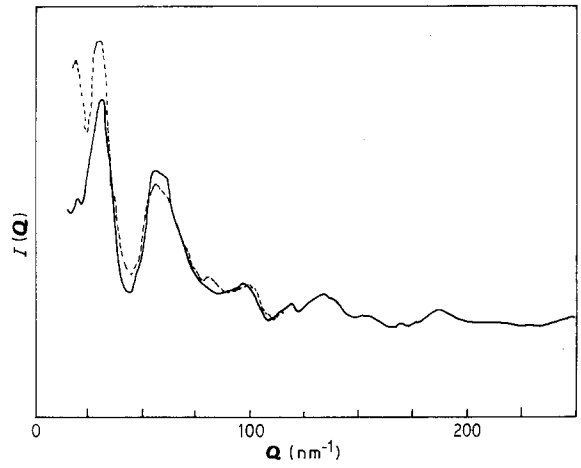


*Figure 5* The scattering data recorded using the geometry of Fig. 3 for a deformed glassy poly(styrene) sample. Solid line, $Q$ perpendicular to extension axis; dashed line, $Q$ parallel to extension axis.

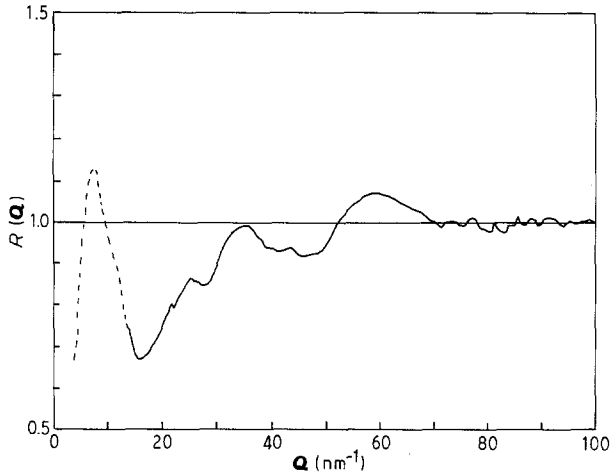


*Figure 6* A plot of the ratio $R(Q)$ of the intensity functions measured with $Q$ perpendicular to the extension axis and with $Q$ parallel to that extension axis for the oriented poly(styrene) glass.

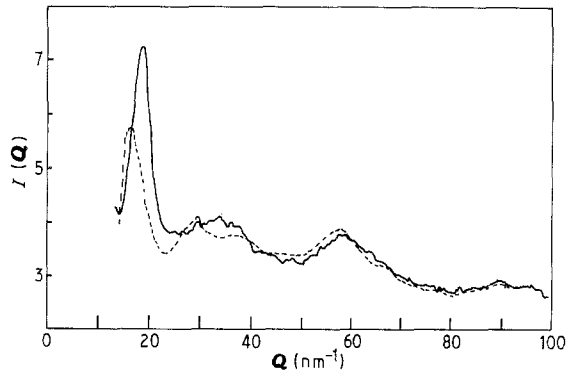


*Figure 7* Neutron-scattering curves for a sample of deuterated poly(pyrrole) prepared using deuterated toluene sulphonate as the counter-ion. The two curves relate to the two detector geometry shown in Fig. 3. Solid line, $Q$ perpendicular to sample surface; dashed line, $Q$ parallel to sample surface.

scattering at $Q \sim 15\,nm^{-1}$ and $30\,nm^{-1}$ is more intense in the direction parallel to the extrusion axis, whereas the scattering at $\sim 8$ and $60\,nm^{-1}$ is more intense in the direction normal to that extension axis. It is noticeable that there is considerable structure in this curve, indicating a diversity of structural origins of the scattering peaks. The peak at $\sim 15\,nm^{-1}$ arises from correlations between neighbouring phenyl groups both within a chain and between chains. The fact that the diffuse peak at $\sim 15\,nm^{-1}$ is more intense when $Q$ is perpendicular to the extension axis suggests that the phenyl groups tend to lie perpendicular to the extension axis. From the sign of the anisotropy of the peak at $Q \sim 8\,nm^{-1}$, the stacks or superchains lie parallel to the extension, which must be so to be consistent with the previous assignment. The diffuse peak at $Q \sim 60\,nm^{-1}$ appears to be dominated by structural correlations between carbon–carbon distances along the chain, as this is more intense with $Q$ parallel to the extension axis. Fig. 6 clearly demonstrates that the technique is able to provide unambiguous and direct structural information pertaining to anisotropy over a substantial $Q$ range. We shall now consider the application of these techniques to a more challenging sample, that of a film of an electrically conducting polymer.

Fig. 7 shows the data recorded using the geometry described in Fig. 3 with the $+/-90°$ detectors for a fully deuterated sample of poly(pyrrole) prepared using deuterated toluene sulphonate as the dopant [20]. That we are able to record this scattering pattern with thin polymer films of thickness $\sim 10\,\mu m$ is a major achievement. The data accumulation time for such samples ranged from 4–8 h. The statistics of these data are not as good as normally obtained for samples of inorganic glasses or molecular fluids, but the scattering does arise from approximately 10 mg of sample. There are clear differences between the two sets of data, although as with poly(styrene), these are minimal for $Q > 100\,nm^{-1}$. In contrast to the scattering from the poly(styrene), for which anisotropy appeared simply as differences in the relative intensities for $Q$ parallel and perpendicular to the extension axis, the poly(pyrrole) sample exhibits distinctly different scattering patterns for curves recorded with $Q$ parallel and perpendicular to the electrode surface. For $Q$ perpendicular to the electrode surface, there is large peak $Q \sim 18\,nm^{-1}$ with the possibility of a second order peak at $35\,nm^{-1}$. These peaks may be related to the closest approach of aromatic rings, thus confirming the notion that the aromatic planes build up on the electrode in an organized manner [18, 19, 23]. The diffuse peak at lower scattering vector for $Q$ parallel to the electrode surface may be related to the more general correlations between neighbouring chain segments. Fig. 8 shows the scattering data recorded for a sample prepared from fully deuterated poly(pyrrole) but with hydrogenated toluene sulphonate as the dopant. It is immediately noticeable that the scattering cross section is higher and there is a pronounced decrease in intensity with increasing $Q$. These effects arise from the presence of a large concentration of hydrogen in the structure. Perhaps the most striking feature is the marked reduction in the height of the peak at $Q \sim 18\,nm^{-1}$ for $Q$ perpendicular to the film surface. This reduction is due to the change in magnitude and sign of the scattering cross-section of the

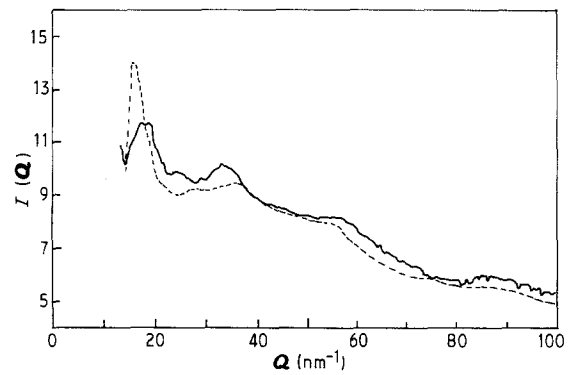


*Figure 8* Neutron-scattering curves for a sample of deuterated poly(pyrrole) prepared using hydrogenated toluene sulphonate as the counter-ion. The two curves relate to the two detector geometry shown in Fig. 3. Solid line, $Q$ perpendicular to the sample surface; dashed line, $Q$ parallel to sample surface.

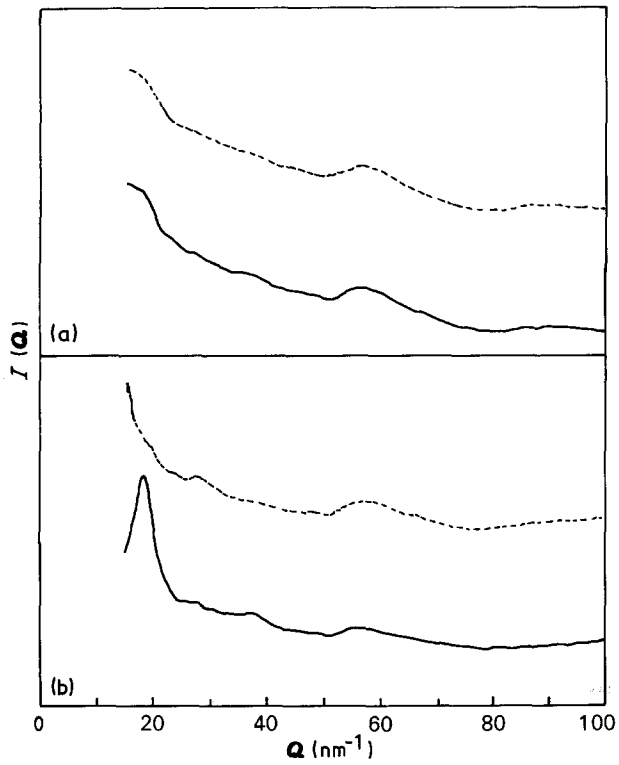


*Figure 9* Comparison of the neutron-scattering curves obtained for samples of deuterated poly(pyrrole) prepared using as counter-ions (a) sulphate and (b) toluene sulphonate, The curves have been offset along the intensity axis. Solid line, $Q$ perpendicular to sample surface; dashed line, $Q$ parallel to sample surface.

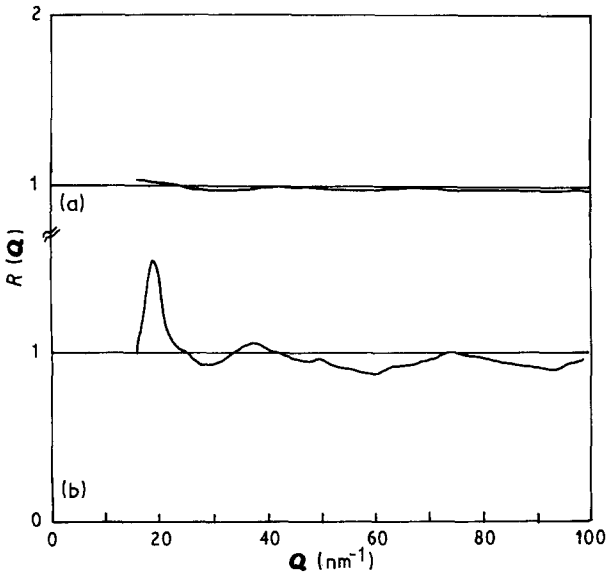


*Figure 10* Plots of the ratios $R(Q)$ of the intensity functions shown in Fig. 9.

hydrogen atoms of the counter-ion unit. The observation that there is a reduction in intensity for this peak for the sample containing the hydrogenated dopant indicates that the dopant units are an integral component of the layered anisotropic structure. In contrast the peak at $Q \sim 15\ nm^{-1}$ remains unaltered by this isotopic substitution, suggesting that few toluene sulphonate units lie in the same plane as the poly(pyrrole) chains. The structure is substantially layered with alternating polymer and dopant layers.

Figs 9 and 10 compare the scattering recorded for two samples of poly(pyrrole), one prepared using toluene sulphonate and one with sulphate. These data, obtained from films synthesized using different dopant units, show that only films prepared with the toluene sulphonate exhibit anisotropy [24].

## 6. Discussion

Although X-ray and neutron-scattering techniques may provide complementary structural information when applied to polymeric systems, there are particular cases in which the neutron can provide new important and unique information which is inaccessible to the X-ray technique. Examples of this are highlighted in this work.

1. The ability of time-of-flight neutron scattering to provide high quality data over an extended $Q$ range, for example $2 < Q < 250\ nm^{-1}$ in a single measurement. Conventional X-ray instruments provide only a limited $Q$ range: for example, flat-film photographic techniques widely employed in fibre diffraction studies have $Q_{max}$ of $30\ nm^{-1}$, whilst for the diffractometer, $Q_{max}$ is typically $65\ nm^{-1}$. The greater $Q$ range offered by neutron time-of-flight scattering is useful in improving the real space resolution (since $\Delta r \sim \pi/Q_{max}$) and in evaluating anisotropy.

2. The possibility of varying the scattering power of the units or sub-units of a structure by isotopic substitution has no counterpart in X-ray scattering. The example given here in respect of the poly(pyrrole) films shows the immense power of this approach of selective deuteration of complex polymer systems.

In this paper we have shown how it is possible to extend these two important advantages by carefully addressing the sample-detector geometries in existing neutron time-of-flight instruments. As a result, we have been able to evaluate directly and swiftly the molecular anisotropy in thin polymeric films. Our techniques enable parallel accumulation of scattering spectra for several orientations of scattering vectors with respect to the anisotropy axis. This parallel data accumulation provides the basic advantage of reducing experimental time and allows thin films to be evaluated on a reasonable time scale. There is certainly no time wasted in stepping the detector through a series of angles. In contrast to X-ray scattering procedures, the examination of thin films is possible with this technique. Conventional X-ray scattering experiments utilize relatively small beams, for example $1 \times 10\ mm^2$ or $1 \times 1\ mm^2$. To maximize the signal from thin films, glancing-angle geometry is usually employed. In the case of neutron scattering, the beam area available is large, for example on LAD 50 $\times 20\ mm^2$. Thin films are usually available with relatively large areas and therefore the whole beam may be employed to effect. This factor considerably eases the geometric problems of evaluating anisotropy. Of course, the parallel data accumulation offers the possibility of evaluating real-time variations in anisotropy, for example liquid-crystal systems in an electric

or magnetic field. In practical terms the measurement time required for current instruments may be too long in comparison to the physical effects to be studied, with polymer relaxation a possible exception. However, for cyclic behaviour, synchronized measurements are a real possibility. The parallel measurements of scattering functions for differing angular relationships between $\boldsymbol{Q}$ and $\alpha$ is also advantageous in reducing any ambiguity which might resulted from either moving the sample or performing data accumulation over different times, as would be employed in the more conventional measurements.

Finally we should consider the evaluation of anisotropy. Following an original suggestion by De Gennes [25], a number of X-ray [12, 26, 27] and neutron [28] studies have utilized the fact that at high $\boldsymbol{Q}$ values the scattering arises from essentially single structural units, and therefore the problems of intermolecular interactions in determining anisotropy from scattering experiments are avoided. The techniques described here not only provide for parallel data accumulation and hence direct anisotropy measurements, but also provide such data over the large $\boldsymbol{Q}$ range essential for these orientation measurement techniques.

## 7. Conclusions

The use of a pulsed neutron source coupled with a novel geometry involving an inclined sample and the use of $+/-90°$ detectors leads directly to a technique which is of considerable utility in the study of anisotropy in thin films. Such anisotropy may be studied over a large scattering-vector range. In addition for polymers and other organic materials, the possibilities of isotopic substitution are powerful in the study of disordered structures, especially of a mixed or complex nature.


## Acknowledgements

This work was supported by the Science and Engineering Research Council and by ICI plc. It is a pleasure to acknowledge the help given by Drs A. C. Hannon and W. S. Howells of the Rutherford Appleton Laboratory with the neutron scattering experiments, and by Dr F. J. Davis of the Polymer Science Centre, University of Reading with the sample preparation.


## References


1. G. KOSTORZ (ed). "Neutron Scattering 15: Treatise on Materials Science and Technology" (Academic, New York, 1979).
2. S. W. LOVESEY, "Theory of Thermal Neutron Scattering" Vols 1 & 2 (Oxford University Press, Oxford, 1985).
3. G. L. SQUIRES, "Introduction to the Theory of Thermal Neutron Scattering" (Cambridge University Press, Cambridge, 1978).
4. R. NEWPORT, B. D. RAINFORD and R. CYWINSKI, "Neutron Scattering at a Pulsed Source" (Adam Hilger, Bristol, 1987).
5. C. G. WINDSOR, "Pulsed Neutron Scattering" (Taylor & Francis, London, 1981).
6. D. M. SADLER, in "Comprehensive Polymer Science" edited by C. Booth & C. Price (Pergamon, Oxford, 1989) ch. 32.
7. A. C. WRIGHT, in "Advances in Structure Research by Diffraction Methods" edited by W. Hoppe & R. Mason (Pergamon, Oxford, 1974) p. 1.
8. G. R. MITCHELL, in "Comprehensive Polymer Science" edited by C. Booth & C. Price (Pergamon, Oxford, 1989) ch. 31.
9. G. R. MITCHELL and R. LOVELL, *Acta Cryst.* **A37** (1981) 189.
10. O. VOGEL, "Textbook of Practical Organic Chemistry" 4th edn. (Longman, London, 1978) p. 642.
11. H. TADOKORO, "Structure of Crystalline Polymers" (Wiley Interscience, New York, 1979) p. 199.
12. G. R. MITCHELL and A. H. WINDLE, *Colloid Polym. Sci.* **260** (1982) 754.
13. W. S. HOWELLS, *J. Phys.* **45** (1984) 81.
14. Rutherford Appleton Laboratory Report RAL-90-041 "User Guide to Experimental Facilities at ISIS" (Rutherford Application Laboratory, Chilton, Didcot, Oxon, U.K. 1990).
15. R. CYWINSKI, Rutherford Appleton Laboratory Report NDR/P15/83 (Rutherford Appleton Laboratory, Chilton, Didcot, Oxon, U.K. 1983).
16. G. R. MITCHELL and A. H. WINDLE, *Polymer* **25** (1984) 906.
17. "Handbook of Conducting Polymers" edited T. A. Skotheim (Dekker, New York, 1986).
18. G. R. MITCHELL, *Polym. Commun.* **27** (1986) 346.
19. G. R. MITCHELL and A. GERI, *J. Phys. D: Appl. Phys.* **20** (1987) 1346.
20. G. R. MITCHELL, F. J. DAVIS, R. CYWINSKI and W. S. HOWELLS, *J. Phys. C: Solid State Phys.* **21** (1988) L411.
21. S. M. WECKER, T. DAVIDSON and J. B. COHEN, *J. Mater. Sci.* **7** (1972) 1249.
22. B. ROSI, G. R. MITCHELL and A. K. SOPER, submitted to *Polym. Commun.*
23. G. R. MITCHELL, F. J. DAVIS and C. H. LEGGE, *Synthetic Metals* **26** (1988) 247.
24. G. R. MITCHELL, F. J. DAVIS, R. CYWINSKI and A. C. HANNON, *Polym. Commun.* **30** (1989) 98.
25. P. G. De GENNES, *C.R. Acad. Sci. (Paris)* **274** (1972) 142.
26. G. R. MITCHELL and A. H. WINDLE, *Polymer* **24** (1983) 1513.
27. G. R. MITCHELL and A. H. WINDLE, in "Crystalline Polymers" edited by D. C. Bassett (Elsevier, London, 1988) Chap. 3.
28. R. PYNN, *J. Phys. Chem.* **34** (1973) 735.



*Received 17 December 1990*
*and accepted 24 April 1991*